Headline Articles

Tetranuclear Mo_2Rh_2 Complexes Obtained from Reactions between Triple Cubane-Type Oxide Cluster $[(Cp^*Rh)_4Mo_4O_{16}]$ ($Cp^* = \eta^5$-$C_5(CH_3)_5$) and Methanethiol: $[\{Cp^*Rh(\mu\text{-}SCH_3)_3MoO_2\}_2(\mu\text{-}O)]$ and $[\{Cp^*Rh(\mu\text{-}SCH_3)_3MoO\}_2(\mu\text{-}X)(\mu\text{-}Y)]$ (X, Y = O and X = O, Y = S). Synthesis, X-Ray Structures, and Dynamic Behavior in Nonaqueous Media

Rimo Xi, Bateer Wang, Masaaki Abe,*,† Yoshiki Ozawa,†† Isamu Kinoshita,††† and Kiyoshi Isobe*,†††

Institute for Molecular Science, Department of Structural Molecular Science, The Graduate University for Advanced Studies, Myodaiji, Okazaki 444-8585

†Division of Chemistry, Graduate School of Science, Hokkaido University, Kita-ku, Sapporo 060-0810

††Department of Material Science, Himeji Institute of Technology, Harima Science Park City, Hyogo 678-1297

†††Department of Material Science, Graduate School of Science, Osaka City University, Sugimoto, Sumiyoshi-ku, Osaka 558-8585

(Received March 25, 1999)

A new series of linear-type Mo_2Rh_2 tetranuclear complexes, $[\{Cp^*Rh^{III}(\mu\text{-}SCH_3)_3Mo^{VI}O_2\}_2(\mu\text{-}O)]$ (**1**), $[\{Cp^*Rh^{III}(\mu\text{-}SCH_3)_3Mo^{V}O\}_2(\mu\text{-}O)_2]$ (**2**), and $[\{Cp^*Rh^{III}(\mu\text{-}SCH_3)_3Mo^{V}O\}_2(\mu\text{-}O)(\mu\text{-}S)]$ (**3**), has been prepared from reactions of the triple cubane-type oxide cluster $[(Cp^*Rh)_4Mo_4O_{16}]\cdot 2H_2O$ with CH_3SH. These tetranuclear complexes have been characterized by elemental analysis, infrared, electronic, and ^1H, ^{13}C, and ^{17}O NMR spectroscopies as well as X-ray analysis.

Complex **1** crystallizes in the monoclinic space group $P2_1/n$ (No. 14) with a = 15.348(3), b = 14.059(3), c = 17.879(3) Å, β = 107.11(2)°, V = 3690(1) Å^3, and Z = 4. Complex **2** crystallizes in the monoclinic space group $C2/c$ (No. 15) with a = 25.334(4), b = 21.271(2), c = 17.831(3) Å, β = 129.70(5)°, V = 7393(2) Å^3, and Z = 8. Complex **3** crystallizes in the orthorhombic space group $Pcab$ (No. 61) with a = 16.902(3), b = 26.631(3), c = 16.855(2) Å, V = 7587(3) Å^3, and Z = 8. Complex **1** involves a nearly linear "$O_2Mo^{VI}(\mu\text{-}O)Mo^{VI}O_2$" framework, to which two Cp^*Rh^{III} units are linked by μ-SCH_3 ligands. Complexes **2** and **3** have an analogous tetranuclear $Mo^{V}{}_2Rh^{III}{}_2$ structure in which the Mo^V and Rh^{III} atoms are bridged by three μ-SCH_3 ligands. Complex **2** contains a doubly-bridged "$OMo^{V}(\mu\text{-}O)_2Mo^{V}O$" framework with an Mo–Mo distance of 2.564(1) Å, while **3** contains a "$OMo^{V}(\mu\text{-}O)(\mu\text{-}S)Mo^{V}O$" framework with an Mo–Mo distance of 2.666(1) Å. Complexes **2** and **3** retain the tetranuclear structure but are fluxional in solution. The fluxional behaviors are due to intramolecular rotations of the "$Cp^*Rh(\mu\text{-}SCH_3)$" moieties on the trigonal planes of the octahedral Mo centers. Line-shape analyses of variable-temperature ^1H NMR spectra measured in C_6D_5Cl yield activation parameters of $\Delta H^{\ddagger}$ = +80.2 kJ mol^{-1}, $\Delta S^{\ddagger}$ = +22.1 J K^{-1} mol^{-1}, and $\Delta G^{\ddagger}_{298\ K}$ = +73.6 kJ mol^{-1} for the rotation in **2** and $\Delta H^{\ddagger}$ = +76.8 kJ mol^{-1}, $\Delta S^{\ddagger}$ = +21.1 J K^{-1} mol^{-1}, and $\Delta G^{\ddagger}_{298\ K}$ = +70.5 kJ mol^{-1} for that in **3**.

Organometallic complexes supported on polyoxoanion surfaces and those incorporated into polyoxoanion frameworks have been extensively studied from interest in their versatile solid-state structures, the unique reactivities, and homogeneous and heterogeneous catalysis.[1—3] During the course of our investigations of organometallic oxide clusters that contain both soft and hard multimetal centers,[4] we isolated and characterized triple cubane-type organometallic oxide clusters, $[(Cp^*M)_4Mo_4^{VI}O_{16}]\cdot nH_2O$, where M = Rh^{III} (n = 2) and Ir^{III} (n = 0).[5] It has been found that the triple cubane rhodium analog reacts with CH_3OH in the presence of p-hydroquinone to yield the incomplete double cubane cluster $[(Cp^*Rh)_2Mo_3O_9(\mu\text{-}OCH_3)_4]$ (Scheme 1a).[6] In this reaction, the cubic M_4O_4 (M = Rh^{III} or Mo^{VI}) framework is maintained and no drastic metal–oxygen bond rearrangements take place. The structure of the incomplete

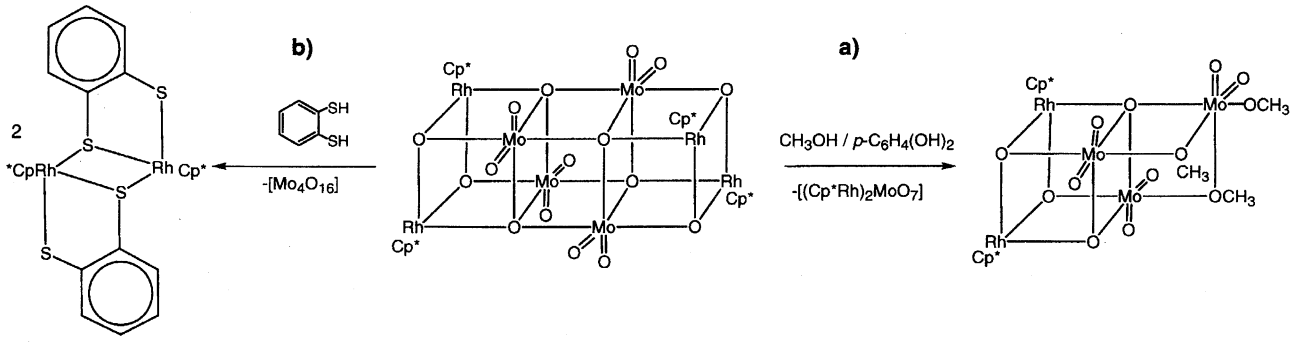

Scheme 1.

cubane cluster suggests that CH_3OH molecules attack the bridging oxygens of $[(Cp^*Rh)_2Mo_4O_{16}]$ to remove formally the "$(Cp^*Rh)_2MoO_7$" part from its framework.[6] On the other hand, even under mild reaction conditions, 1,2-benzenedithiol induces a complete reconstruction of the cluster framework to separate the organorhodium and oxide parts with formation of $[(Cp^*Rh)_2(\mu(S)\text{-}1,2\text{-}C_6H_4S_2\text{-}S,S')_2]$ (Scheme 1b).[7]

In an extension of our study to the reaction using CH_3SH as the substrate, we have found that the transformation of the framework of the triple cubane cluster varies with reaction conditions such as solvent, reaction temperature, and the concentrations of the cluster and thiol as described in our communications[8,9] and note.[10] The reaction in CH_3CN in the presence of a high concentration of CH_3SH produces $[(Cp^*Rh)_2(\mu\text{-}SCH_3)_3]_4[Mo_8O_{26}]$[10] and $[(Cp^*Rh)_2(\mu\text{-}SCH_3)_3]_2[Mo_6O_{19}]$[11] in which the organorhodium and oxomolybdate moieties are completely separated. The reactions in CH_2Cl_2 at room temperature, in CH_3OH using the vapor of CH_3SH at room temperature, and in CH_3OH under refluxing conditions give the Mo_2Rh_2 tetranuclear complexes of $[\{Cp^*Rh^{III}(\mu\text{-}SCH_3)_3Mo^{VI}O_2\}_2(\mu\text{-}O)]$ (**1**),[8] $[\{Cp^*Rh^{III}(\mu\text{-}SCH_3)_3Mo^{V}O\}_2(\mu\text{-}O)_2]$ (**2**),[9] and $[\{Cp^*Rh^{III}(\mu\text{-}SCH_3)_3Mo^{V}O\}_2(\mu\text{-}O)(\mu\text{-}S)]$ (**3**),[9] respectively, together with the octa- and hexa- molybdates as main products. In this paper, we will describe the full account of (i) the reactions of $[(Cp^*Rh)_4Mo_4O_{16}]$ with CH_3SH to give the Mo_2Rh_2 tetranuclear complexes of **1**, **2**, and **3**, and (ii) the structural and bonding study of these products based on the results of X-ray analysis, and (iii) the elucidation of the fluxional behaviors of **2** and **3** using complete line-shape analyses of variable-temperature ^1H NMR spectra. The ^{17}O-enriched analogs were also prepared and characterized by ^{17}O NMR spectroscopy.

Experimental

Materials. The starting compounds of $[\{Cp^*RhCl(\mu\text{-}Cl)\}_2]$ [12] and $[(Cp^*Rh)_4Mo_4O_{16}]\cdot 2H_2O$ [5] were prepared according to the literature methods. The following chemicals were purchased from commercial sources and used without further purification: $RhCl_3\cdot 3H_2O$ (Shiga Kikinzoku), $Na_2MoO_4\cdot 2H_2O$ (Wako), pentamethylcyclooctadiene (Kanto Kagaku), CH_3SH (30% in CH_3OH) (Nacalai), and 10% ^{17}O-enriched water (CEA). The solvents of CH_3OH and CH_2Cl_2 were distilled under Ar. Other solvents were used as received.

Preparation of Tetranuclear Mo_2Rh_2 Complexes. $[\{Cp^*Rh(\mu\text{-}SCH_3)_3MoO_2\}_2(\mu\text{-}O)]$ (1). To a solution of CH_3SH (3.0 cm^3: 30% in CH_3OH, 15 mmol) in CH_2Cl_2 (10 cm^3) was added dropwise a solution of $[(Cp^*Rh)_4Mo_4O_{16}]\cdot 2H_2O$ [5] (0.35 g, 0.21 mmol) in CH_2Cl_2 (15 cm^3) at room temperature. After the mixture was stirred for 30 min, the solvent was evaporated. The orange residue was dissolved in a minimum quantity of CH_2Cl_2 and the insoluble yellow solid of polyoxometalates[13] was removed by filtration. The filtrate was treated with a column chromatography of silica gel with $CH_2Cl_2/(CH_3)_2CO$ (acetone) (15/1, v/v) as an eluent. The first fraction was evaporated to give **1** as an orange solid in a 20% yield (90 mg). Complex **1** was also obtained by using CH_3OH as the solvent, but in a much lower yield. Single crystals suitable for X-ray analysis were grown from a CH_3CN solution at room temperature. Anal. Calcd for $C_{26}H_{48}Mo_2O_5Rh_2S_6$: C, 30.30; H, 4.69%. Found: C, 30.56; H, 4.68%. Negative ion FAB MS (NBA as a matrix): the most intense peak, m/z = 1030 ($[M]^-$). IR (KBr pellet, cm^{-1}, 1100—700 cm^{-1} region) ν(Mo–O_t): 1023 (m), 951 (m), 919 (s), 891 (s); ν(Mo–O_b): 750 (s) (O_t and O_b represent the terminal and the bridging oxygen atoms, respectively). ^1H NMR ($CDCl_3$, 23 °C, δ vs. TMS) δ = 2.22 (s, br, SCH_3), 2.19 (s, br, SCH_3), 2.17 (s, br, SCH_3), 2.03 (s, br, SCH_3), 1.95 (s, br, SCH_3), 1.78 (s, 30H, $C_5(CH_3)_5$). $^{13}C\{^1H\}$ NMR ($CDCl_3$, 23 °C, δ vs. TMS) δ = 97.3 (d, J_{Rh-C} = 6.1 Hz, $C_5(CH_3)_5$), 15.3 (s, SCH_3), 13.8 (s, SCH_3), 13.6 (s, SCH_3), 12.9 (s, SCH_3), 9.4 (s, $C_5(CH_3)_5$). Electronic spectrum (CH_2Cl_2, 25 °C) λ_{max} (ε/M^{-1} cm^{-1}), ca. 370 (sh), 300 (3.3×10^4), 246 (4.4×10^4) (M = mol dm^{-3}, sh = shoulder). The second fraction of the chromatography gave complex **2** (yield, 40 mg: 9%, see below).

$[\{Cp^*Rh(\mu\text{-}SCH_3)_3MoO\}_2(\mu\text{-}O)_2]$ (2). A solution of $[(Cp^*Rh)_4Mo_4O_{16}]\cdot 2H_2O$ [5] (0.60 g, 0.37 mmol) in CH_3OH (60 cm^3) was stirred at room temperature and was allowed to react gradually with the vapor of CH_3SH (30 cm^3, 1.5×10^2 mmol) introduced into a reaction flask through a glass tube with glass wool. After one week, red crystals of **2** and yellow orange solid of polyoxometalates[13] were deposited. The red crystals were collected by filtration and hand, washed with diethyl ether, and dried in vacuo. Yield, 140 mg (19%). The deposited red crystals were used for X-ray analysis. Anal. Calcd for $C_{26}H_{48}Mo_2O_4Rh_2S_6$: C, 30.78; H, 4.77%. Found: C, 30.96; H, 4.76%. Negative ion FAB MS (NBA as a matrix): the most intense peak, m/z = 1014 ($[M]^-$). IR (KBr pellet, cm^{-1}, 1100—700 cm^{-1} region) ν(Mo–O_t): 940 (s), 923 (m); ν(Mo–O_b): 724 (m), 708 (m), 446 (m). ^1H NMR ($CDCl_3$, 23 °C, δ vs. TMS) δ = 2.54 (s, 6H, SCH_3), 2.20 (s, 6H, SCH_3), 1.81 (s, 30H, $C_5(CH_3)_5$), 1.60 (s, 6H, SCH_3). $^{13}C\{^1H\}$ NMR ($CDCl_3$, 23 °C, δ vs. TMS) δ = 96.9 (d, J_{Rh-C} = 6.1 Hz, $C_5(CH_3)_5$), 17.3 (s, SCH_3), 13.0 (s, SCH_3), 12.5 (s, SCH_3), 9.4 (s, $C_5(CH_3)_5$). Electronic spectrum (CH_2Cl_2, 25 °C) λ_{max} (ε/M^{-1} cm^{-1}), 370 (sh), 330

(sh), 310 (sh), 295 (4.3×10^4), 249 (5.5×10^4).

[{Cp*Rh(μ-SCH$_3$)$_3$MoO}$_2$(μ-O)(μ-S)] (3). A solution of [(Cp*Rh)$_4$Mo$_4$O$_{16}$]·2H$_2$O [5] (0.20 g, 0.12 mmol) in CH$_3$OH (20 cm^3) was added to a solution of CH$_3$SH (5.0 cm^3, 25 mmol). The mixture was refluxed for 1 h under an Ar atmosphere. The mixture was cooled down to room temperature and the resulting yellow solid of polyoxometalates[13] was removed by filtration. The filtrate was evaporated to dryness to leave an orange residue. The residue was dissolved in a small amount of CH$_2$Cl$_2$, and it was subjected to a column chromatography of silica gel with elution by CH$_2$Cl$_2$/(CH$_3$)$_2$CO (15/1, v/v). An orange solid **3** was isolated from the major orange band on the column. Yield, 44 mg (17%). Single crystals of **3** suitable for X-ray analysis were grown from a CH$_2$Cl$_2$ solution at room temperature. Anal. Calcd for C$_{26}$H$_{48}$Mo$_2$O$_3$Rh$_2$S$_7$: C, 30.30; H, 4.69%. Found: C, 30.04; H, 4.56%. Negative ion FAB MS (NBA as a matrix): the most intense peak, m/z = 1030 ([M]$^-$). IR (KBr pellet, cm^{-1}, 1100—700 cm^{-1} region) ν(Mo–O$_t$): 948 (sh), 927 (s); ν(Mo–O$_b$): 708 (m); ν(Mo–S$_b$): 494 (m). ^{1}H NMR (CDCl$_3$, 23 °C, δ vs. TMS) δ = 2.60 (s, 3H, SC*H*$_3$), 2.51 (s, 3H, SC*H*$_3$), 2.47 (s, 3H, SC*H*$_3$), 2.27 (s, 3H, SC*H*$_3$), 1.80 (s, 30H, C$_5$(C*H*$_3$)$_5$), 1.57 (s, 3H, SC*H*$_3$), 1.55 (s, 3H, SC*H*$_3$). ^{13}C{^{1}H} NMR (CDCl$_3$, 23 °C, δ vs. TMS) δ = 96.8 (d, J_{Rh-C} = 6.1 Hz, *C*$_5$(CH$_3$)$_5$), 18.7 (s, S*C*H$_3$), 17.5 (s, S*C*H$_3$), 16.4 (s, S*C*H$_3$), 15.0 (s, S*C*H$_3$), 13.6 (s, S*C*H$_3$), 12.8 (s, S*C*H$_3$), 9.4 (s, C$_5$(*C*H$_3$)$_5$). Electronic spectrum (CH$_2$Cl$_2$, 25 °C) λ_{max} (ε/M^{-1} cm^{-1}), 370 (sh), 330 (sh), 294 (3.1×10^4), 256 (4.8×10^4).

Reaction of 1 with CH$_3$SH. A solution of complex **1** (0.15 g, 0.15 mmol) in CH$_2$Cl$_2$ (10 cm^3) was combined with a solution of CH$_3$SH (0.5 cm^3, 2.5 mmol) in CH$_3$OH (10 cm^3), and the mixture was refluxed for 12 h. The resultant solution was cooled down to room temperature and the solvent was removed by evaporation. The residue was dissolved in a minimum amount of CH$_2$Cl$_2$ and the insoluble material of polyoxometalates[13] was filtered off. The filtrate was subjected to silica gel column chromatography with CH$_2$Cl$_2$/(CH$_3$)$_2$CO (15/1, v/v) as an eluent. The first and the second fractions gave complexes **3** and **2**, respectively. Yield: complex **2**, 35 mg (24%); complex **3**, 30 mg (20%).

^{17}O-Enrichment Procedures. [(Cp*Rh)$_4$Mo$_4$(^{17}O)$_{16}$]·2H$_2$^{17}O. A suspension of Na$_2$MoO$_4$·2H$_2$O (1.40 g, 5.79 mmol) in 10% H$_2$^{17}O (1.5 cm^3) was stirred at 40 °C for 2 h under an Ar atmosphere. To the resulting solution were added [{Cp*RhCl(μ-Cl)}$_2$] (1.00 g, 1.62 mmol) and H$_2$O (1.5 cm^3), and then the mixture was vigorously stirred at 90 °C for 10 h. An orange residue was obtained by evaporation of the solvent, and it was extracted with CH$_2$Cl$_2$ (150 cm^3). The extract was dried over Na$_2$SO$_4$ for 12 h. The ^{17}O-enriched sample, [(Cp*Rh)$_4$Mo$_4$(^{17}O)$_{16}$]·2H$_2$^{17}O, was obtained in 73% yield (based on the Rh atom, 970 mg) by evaporation of the solvent.

^{17}O-Enriched Samples of [{Cp*Rh(μ-SCH$_3$)$_3$Mo^{17}O$_2$}$_2$(μ-^{17}O)] (1′), [{Cp*Rh(μ-SCH$_3$)$_3$Mo^{17}O}$_2$(μ-^{17}O)$_2$] (2′), and [{Cp*Rh(μ-SCH$_3$)$_3$Mo^{17}O}$_2$(μ-^{17}O)(μ-S)] (3′). To a solution of CH$_3$SH (3.0 cm^3, 15 mmol) in CH$_2$Cl$_2$ (10 cm^3) was added a solution of ^{17}O-enriched [(Cp*Rh)$_4$Mo$_4$^{17}O$_{16}$]·2H$_2$O (0.20 g, 0.12 mmol), in CH$_2$Cl$_2$ (15 cm^3) at room temperature. After the mixture was stirred for 30 min, the solvent was removed by evaporation, and the residue was treated with column chromatography of silica gel using a mixture of CH$_2$Cl$_2$/(CH$_3$)$_2$CO (15/1, v/v) as an eluent. Complexes **1′** and **2′** were obtained from the first (yield: 53 mg, 21%) and the second fraction (yield: 32 mg, 13%), respectively, after evaporation of the solvent. Complex **3′** was obtained by a similar manner to that for **3** (yield: 40 mg, 16%).

Measurements. Elemental analysis and mass spectral measurements were performed at the Chemical Material Center in the Institute for Molecular Science and the Chemical Analysis Service Laboratory in Osaka City University. Infrared spectra were obtained with the KBr method on a Perkin Elmer 1600 series FT-IR spectrophotometer. Negative FAB mass spectra were measured with a Shimadzu/Kratos CONCEPT 1S mass spectrometer. Absorption spectra were recorded on a Hitachi U-3400 spectrophotometer. ^{1}H (400.0 MHz), ^{13}C{^{1}H} (100.5 MHz), and ^{17}O (54.2 MHz) NMR spectra were obtained in a JEOL GX-400 NMR spectrometer equipped with a variable-temperature controller. Samples were allowed to stand for at least ten minutes before spectra were recorded at desired temperatures, in order to get their equilibrium states. Chemical shifts were referenced to TMS for ^{1}H and ^{13}C{^{1}H} NMR spectra. In the case of ^{17}O NMR, chemical shifts were referenced to D$_2$O externally by the sample replacement method. Typical ^{17}O spectral parameters are, the spectrometer frequency = 54.2 MHz, the pulse delay = 100 μs, the predelay = 0.2 ms, and the pulse width = 7.5 μs.

X-Ray Structural Determinations. [{Cp*Rh(μ-SCH$_3$)$_3$-MoO$_2$}$_2$(μ-O)] (1). An orange prismatic single crystal of **1** was mounted on a Rigaku AFC-5 four-circle diffractometer. A total of 11637 reflections were collected at 25 °C with graphite-monochromated Mo $K\alpha$ radiation (λ = 0.71073 Å) using the θ–2θ scan technique in the $2° < 2\theta < 60°$ range. The cell dimensions were determined by least-squares fitting of 25 centered reflections ($25° < 2\theta < 30°$). Three standard reflections measured periodically throughout data collection revealed negligible decay for all three complexes. The intensity data were corrected for Lorentz-polarization factors and the absorption effect (numerical Gaussian integration method). The structure was solved by Patterson methods using SHELXS-86[14a] and refined with a block-diagonal least squares technique using UNICS III[14b] program on a HITAC M680 computer at the Institute for Molecular Science Computer Center. Space group $P2_1/n$ was confirmed by subsequent successful structural solution and refinement. Hydrogen atoms were not included in the refinement.

[{Cp*Rh(μ-SCH$_3$)$_3$MoO}$_2$(μ-O)$_2$] (2). A red prismatic single crystal of **2** was mounted on a Rigaku AFC-5 four-circle diffractometer. A total of 11088 reflections were collected at 25 °C with graphite-monochromated Mo $K\alpha$ radiation (λ = 0.71073 Å) using the θ–2θ scan technique in the $2° < 2\theta < 60°$ range. The cell dimensions were determined by least-squares fitting of 25 centered reflections ($25° < 2\theta < 30°$). The intensity data were corrected for Lorentz-polarization factors and the absorption effect. The structure solution and refinement were carried out by the same method as that for **1**.

[{Cp*Rh(μ-SCH$_3$)$_3$MoO}$_2$(μ-O)(μ-S)] (3). A red prismatic single crystal of **3** was mounted on a Rigaku AFC-5 four-circle diffractometer. A total of 9679 reflections were collected at 25 °C with graphite-monochromated Mo $K\alpha$ radiation (λ = 0.71073 Å) using the θ–2θ scan technique in the $2° < 2\theta < 55°$ range. The cell dimensions were determined by least-squares fitting of 25 centered reflections ($25° < 2\theta < 30°$). The structure solution and refinement were carried out by the same method as that for **1**.

Crystallographic data of the above three complexes have been deposited at the CCDC, 12 Union Road, Cambridge CB2 1EZ, UK and copies can be obtained on request, free of charge, by quoting the publication and the deposition numbers CCDC 128211, 128212, and 128213.

Line-Shape Analysis of Variable-Temperature ^{1}H NMR Spectra. Line-shape analysis of variable-temperature ^{1}H NMR spectra

for complexes **2** and **3** was carried out using a computer program based on a modified Bloch equation with the three-site exchange model.[15] Rate constants were determined by visual fitting of observed and calculated spectra. Activation parameters were calculated from the Eyring plots.

Results and Discussion

Reaction of $[(Cp^*Rh)_4Mo_4O_{16}]\cdot 2H_2O$ with CH_3SH. Three linear-type Rh_2Mo_2 tetranuclear complexes, $[\{Cp^*Rh(\mu\text{-}SCH_3)_3MoO_2\}_2(\mu\text{-}O)]$ (**1**), $[\{Cp^*Rh(\mu\text{-}SCH_3)_3MoO\}_2(\mu\text{-}O)_2]$ (**2**), and $[\{Cp^*Rh(\mu\text{-}SCH_3)_3MoO\}_2(\mu\text{-}O)(\mu\text{-}S)]$ (**3**) are obtained from the reactions of the triple cubane-type cluster, $[(Cp^*Rh)_4Mo_4O_{16}]\cdot 2H_2O$,[5] with excess CH_3SH in organic solvents. The formations of the singly-bridged μ-oxo complex **1** (20% yield) and doubly-bridged di(μ-oxo) complex **2** (9% yield) are observed in CH_2Cl_2 under the relatively mild conditions, while doubly-bridged (μ-oxo)(μ-sulfido) complex **3** is obtained when $[(Cp^*Rh)_4Mo_4O_{16}]\cdot 2H_2O$ is reacted with CH_3SH at higher temperature (refluxing CH_3OH). These results indicate that the reactions with CH_3SH cause more drastic rearrangements of the cubic framework than that with CH_3OH. Although the reactions with CH_3SH also produced the byproducts of the previously characterized octamolybdate $[(Cp^*Rh)_2(\mu\text{-}SCH_3)_3]_4[Mo_8O_{26}]$ [10] and hexamolybdate $[(Cp^*Rh)_2(\mu\text{-}SCH_3)_3]_2[Mo_6O_{19}]$ [11] where the Rh and Mo moieties are separated, its affinity for the Rh atom seems to be weaker than that of $1,2\text{-}C_6H_4(SH)_2$ which gives quantitatively the completely rearranged product of $[(Cp^*Rh)_2(\mu(S)\text{-}1,2\text{-}C_6H_4S_2\text{-}S,S')_2]$,[7] since the reaction of CH_3SH gives the Rh_2Mo_2 tetranuclear complexes of **1**—**3** under certain reaction conditions, which are severer than those employed in the reaction of $1,2\text{-}C_6H_4(SH)_2$.

Lower yields of the tetranuclear complexes, **1**—**3**, are due to the simultaneous formations of the octamolybdate and hexamolybdate. The reaction sequence is shown in

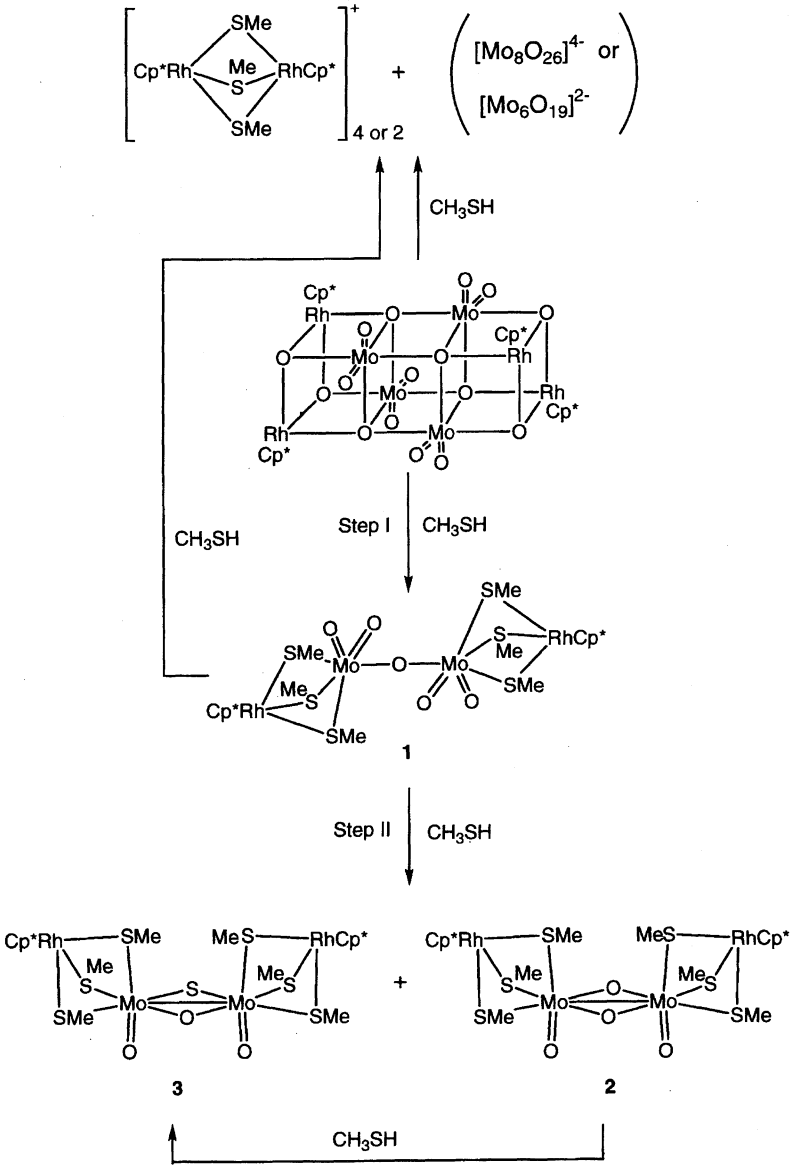

Scheme 2.

Scheme 2. We propose that these tetranuclear complexes are mainly formed through two steps (Steps I and II) which are described as Eqs. 1 and 2, where complex **1** is a key intermediate. The first step involves the destruction of the triple cubane core by CH_3SH, followed by the reconstruction into the singly-bridged tetranuclear of **1** (Eq. 1).

$$[(Cp^*Rh^{III})_4Mo_4^{VI}O_{16}]\cdot 2H_2O + 12CH_3SH \longrightarrow 2[\{Cp^*Rh^{III}(\mu\text{-}SCH_3)_3Mo^{VI}O_2\}_2(\mu\text{-}O)](\mathbf{1}) + 8H_2O \quad (1)$$

The second step is the formation of doubly-bridged species **2** and **3** through the reaction of **1** with CH_3SH which plays a role as a reductant of Mo^{VI} in **1** to Mo^{V} in **2** and **3** and as a sulfide source for **3** (Eq. 2).[16]

$$2[\{Cp^*Rh^{III}(\mu\text{-}SCH_3)_3Mo^{VI}O_2\}_2(\mu\text{-}O)](\mathbf{1}) + 6CH_3SH \longrightarrow [\{Cp^*Rh^{III}(\mu\text{-}SCH_3)_3Mo^{V}O\}_2(\mu\text{-}O)_2](\mathbf{2}) + [\{Cp^*Rh^{III}(\mu\text{-}SCH_3)_3Mo^{V}O\}_2(\mu\text{-}O)(\mu\text{-}S)](\mathbf{3}) + 2(CH_3S)_2 + (CH_3)_2S + 3H_2O \quad (2)$$

This scheme is supported by the observation that **2** and **3** can be generated by the reaction of complex **1** with CH_3SH. Complex **3** was also detected in a prolonged reaction of **2** with CH_3SH. The octamolybdate[10] and hexamolybdate[11] salts are generated from both the triple cubane cluster and complex **1**. The core rearrangements by CH_3SH may be explained by the high reactivity of the soft sulfur atom in CH_3SH towards the metal ions (particularly the Rh^{III} atoms) in the triple cubane cluster. In addition, the more acidic nature of CH_3SH,[17] compared with CH_3OH, would accelerate protonation to the bridging oxygen sites, leading to the easier metal–oxygen bond cleavage in the cluster.

Of particular interest in the formation of **3** is that the bridging sulfur atom is introduced by the cleavage of the S–C bond, similar to that seen in the desulfurization process.[18] It is noted that the doubly sulfido-bridged analogs or those having terminal sulfur ligand(s) have not been detected under the present conditions. Although many dinuclear molybdenum complexes having the frameworks of "O_2Mo^{VI}-(μ-O)$Mo^{VI}O_2$", "$OMo^{V}(\mu\text{-}O)_2Mo^{V}O$", and "$OMo^{V}(\mu$-O)-($\mu$-S)$Mo^{V}O$" have been prepared to date,[19] the complexes with additional metal complex groups on their frameworks like **1**—**3** are rare except for the cubane-type clusters[19e] and [{(tiptacn)MoO(μ-O)$_2$}$_2$Mo(bpy)](PF$_6$)$_2$ (tiptacn = 1,4,7-triisopropyl-1,4,7-triazacyclononane)[20] and several other oligomeric complexes[19i] based on the "$OMo^{V}(\mu\text{-}O)_2Mo^{V}O$" cores.

Description of Structures. The tetranuclear structures of [{Cp*Rh(μ-SCH$_3$)$_3$MoO$_2$}$_2$(μ-O)] (**1**), [{Cp*Rh(μ-SCH$_3$)$_3$MoO}$_2$(μ-O)$_2$] (**2**), and [{Cp*Rh-(μ-SCH$_3$)$_3$MoO}$_2$(μ-O)(μ-S)] (**3**), have been unambiguously determined by single-crystal X-ray crystallography. A summary of crystallographic data is given in Table 1 and selected interatomic distances and angles are presented in Table 2. Other structural data are described in Supporting Information. The ORTEP drawings of **1**, **2**, and **3** are displayed in Figs. 1, 2, and 3, respectively.

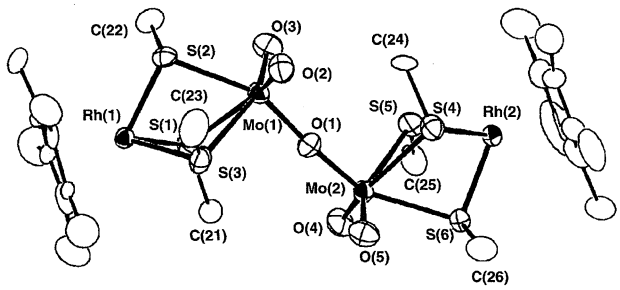

Fig. 1. An ORTEP drawing (50% ellipsoids) of [{Cp*Rh-(μ-SCH$_3$)$_3$MoO$_2$}$_2$(μ-O)] (**1**) with atomic labeling scheme.

Table 1. Crystallographic Data and Refinement Parameters for **1**, **2**, and **3**

	1	**2**	**3**
Formula	$C_{26}H_{48}Mo_2O_5Rh_2S_6$	$C_{26}H_{48}Mo_2O_4Rh_2S_6$	$C_{26}H_{48}Mo_2O_3Rh_2S_7$
F_w	1030.72	1014.72	1030.78
Cryst system	Monoclinic	Monoclinic	Orthorhombic
Space group	$P2_1/n$ (No. 14)	$C2/c$ (No. 15)	$Pcab$ (No. 61)
Temp/°C	25	25	25
a/Å	15.348(3)	25.334(4)	16.902(3)
b/Å	14.059(3)	21.271(2)	26.631(3)
c/Å	17.879(3)	17.831(3)	16.855(2)
β/deg	107.11(2)	129.70(5)	90
V/Å^3	3690(1)	7393(2)	7587(3)
Z	4	8	8
Cryst dimens/mm^3	0.40 × 0.35 × 0.25	0.48 × 0.38 × 0.21	0.43 × 0.33 × 0.23
λ(Mo $K\alpha$)/Å	0.71073	0.71073	0.71073
d_{calcd}/g cm^{-3}	1.855	1.823	1.805
μ/cm^{-1}	18.73	18.67	18.70
Data collcd	11637	11088	9679
Independent data	2378	8807	5015
R[a]	0.064	0.045	0.044
R_w[b]	0.065	0.090	0.055

a) $R = \sum||F_o| - |F_c||/\sum|F_o|$. b) $R_w = [\sum|w(|F_o| - |F_c|)^2)/\sum|w|F_o|^2]^{1/2}$; $w^{-1} = \sigma(F_o)^2 + (0.020F_o)^2$.

Table 2. Selected Interatomic Distances (Å) and Angles (°) of **1**, **2**, and **3**

Complex **1**			
	Distances (Å)		
Rh(1)···Mo(1)	3.520(3)	Rh(2)···Mo(2)	3.526(3)
Mo(1)–O(1)	1.91(1)	Mo(2)–O(1)	1.86(1)
Mo(1)–O(2)	1.70(2)	Mo(2)–O(4)	1.71(2)
Mo(1)–O(3)	1.70(2)	Mo(2)–O(5)	1.66(2)
Rh(1)–S(1)	2.359(6)	Rh(2)–S(4)	2.362(6)
Rh(1)–S(2)	2.327(6)	Rh(2)–S(5)	2.362(7)
Rh(1)–S(3)	2.348(7)	Rh(2)–S(6)	2.338(6)
Mo(1)–S(1)	2.689(7)	Mo(2)–S(4)	2.720(7)
Mo(1)–S(2)	2.554(6)	Mo(2)–S(5)	2.682(6)
Mo(1)–S(3)	2.691(7)	Mo(2)–S(6)	2.553(6)
C(23)···O(2)	3.12(3)	C(25)···O(4)	3.08(3)
C(22)···O(3)	3.02(3)	C(26)···O(5)	2.96(3)
	Angles (deg)		
Mo(1)–O(1)–Mo(2)	175(1)		
S(1)–Mo(1)–S(2)	70.9(2)	S(4)–Mo(2)–S(5)	69.3(2)
S(1)–Mo(1)–S(3)	69.7(2)	S(4)–Mo(2)–S(6)	70.5(2)
S(2)–Mo(1)–S(3)	70.7(2)	S(5)–Mo(2)–S(6)	71.9(2)
O(1)–Mo(1)–O(2)	104.4(8)	O(1)–Mo(2)–O(4)	105.8(8)
O(1)–Mo(1)–O(3)	105.0(7)	O(1)–Mo(2)–O(5)	104.3(7)
O(2)–Mo(1)–O(3)	105.4(8)	O(4)–Mo(2)–O(5)	107.0(8)
Complex **2**			
	Distances (Å)		
Mo(1)–Mo(2)	2.564(1)		
Rh(1)···Mo(1)	3.466(2)	Rh(2)···Mo(2)	3.471(1)
Mo(1)–S(1)	2.736(3)	Mo(2)–S(4)	2.704(3)
Mo(1)–S(2)	2.569(2)	Mo(2)–S(5)	2.615(3)
Mo(1)–S(3)	2.583(3)	Mo(2)–S(6)	2.548(2)
Mo(1)–O(1)	1.938(5)	Mo(2)–O(1)	1.919(4)
Mo(1)–O(4)	1.948(5)	Mo(2)–O(4)	1.951(5)
Mo(1)–O(2)	1.704(10)	Mo(2)–O(3)	1.703(9)
Rh(1)–S(1)	2.351(2)	Rh(2)–S(4)	2.353(2)
Rh(1)–S(2)	2.391(3)	Rh(2)–S(5)	2.370(3)
Rh(1)–S(3)	2.359(3)	Rh(2)–S(6)	2.376(3)
C(21)···O(1)	3.23(2)	C(22)···O(4)	3.27(1)
C(23)···O(2)	3.05(1)	C(24)···O(4)	3.07(2)
C(25)···O(3)	2.99(1)	C(26)···O(1)	3.08(1)
	Angles (deg)		
S(1)–Mo(1)–S(2)	70.38(8)	S(4)–Mo(2)–S(5)	70.84(8)
S(1)–Mo(1)–S(3)	71.59(9)	S(4)–Mo(2)–S(6)	71.69(8)
S(2)–Mo(1)–S(3)	75.20(6)	S(5)–Mo(2)–S(6)	74.31(6)
O(1)–Mo(1)–O(4)	93.5(2)	O(1)–Mo(2)–O(4)	94.0(2)
O(1)–Mo(1)–O(2)	109.6(3)	O(1)–Mo(2)–O(3)	109.2(3)
Complex **3**			
	Distances (Å)		
Mo(1)–Mo(2)	2.666(1)		
Rh(1)···Mo(1)	3.480(1)	Rh(2)···Mo(2)	3.477(1)
Mo(1)–S(1)	2.717(2)	Mo(2)–S(4)	2.734(2)
Mo(1)–S(2)	2.558(3)	Mo(2)–S(5)	2.589(2)
Mo(1)–S(3)	2.594(2)	Mo(2)–S(6)	2.556(2)
Mo(1)–O(1)	1.937(5)	Mo(2)–O(1)	1.948(6)
Mo(1)–S(7)	2.335(3)	Mo(2)–S(7)	2.327(2)
Mo(1)–O(2)	1.688(6)	Mo(2)–O(3)	1.689(6)
Rh(1)–S(1)	2.372(2)	Rh(2)–S(4)	2.362(2)
Rh(1)–S(2)	2.370(3)	Rh(2)–S(5)	2.360(2)
Rh(1)–S(3)	2.368(2)	Rh(2)–S(6)	2.379(2)
C(21)···O(1)	3.14(1)	C(22)···S(7)	3.37(1)
C(23)···O(2)	3.01(1)	C(24)···S(7)	3.41(2)
C(25)···O(3)	3.04(1)	C(26)···O(1)	3.05(1)
	Angles (deg)		
S(1)–Mo(1)–S(2)	70.78(8)	S(4)–Mo(2)–S(5)	69.78(7)
S(1)–Mo(1)–S(3)	71.01(7)	S(4)–Mo(2)–S(6)	70.44(7)
S(2)–Mo(1)–S(3)	74.73(8)	S(5)–Mo(2)–S(6)	75.98(7)
O(1)–Mo(1)–S(7)	98.4(2)	O(1)–Mo(2)–S(7)	98.3(2)
O(1)–Mo(1)–O(2)	106.8(3)	O(1)–Mo(2)–O(3)	107.5(3)
O(2)–Mo(1)–S(7)	107.6(2)	O(3)–Mo(2)–S(7)	107.3(2)

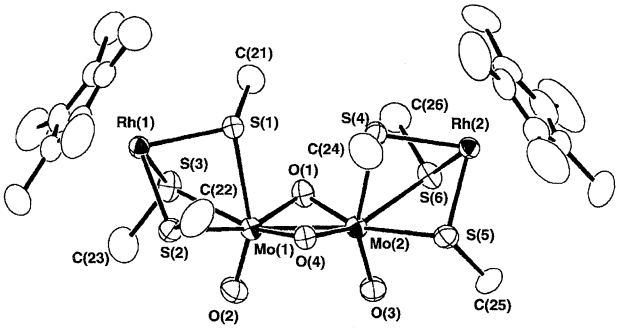

Fig. 2. An ORTEP drawing (50% ellipsoids) of [{Cp*Rh-(μ-SCH_3)$_3$MoO}$_2$(μ-O)$_2$] (**2**) with atomic labeling scheme.

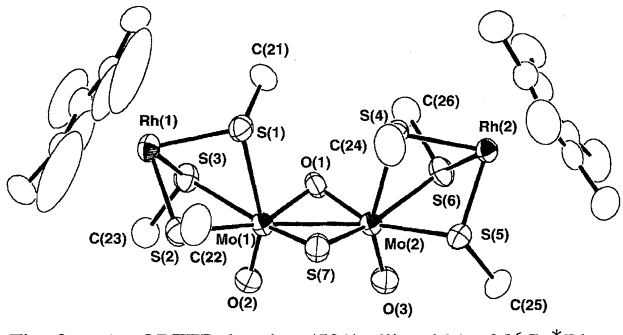

Fig. 3. An ORTEP drawing (50% ellipsoids) of [{Cp*Rh-(μ-SCH_3)$_3$MoO}$_2$(μ-O)(μ-S)] (**3**) with atomic labeling scheme.

Molecular Structure of 1. As seen in Fig. 1, complex **1** consists of a singly oxo-bridged dioxodimolybdenum(VI) core $O_2Mo^{VI}(\mu\text{-}O)Mo^{VI}O_2$ and two Cp*Rh fragments that are linked to the Mo centers by three μ-SCH_3 bridges. The geometry of two "Cp*Rh(μ-SCH_3)$_3$$MoO_2$" groups takes a transoid configuration around the nearly linear Mo–(μ-O)–Mo axis (175(1)°), which would be caused by steric crowding of the two bulky moieties. Such a transoid configuration has been found in the (μ-oxo)dimolybdenum(VI) complexes, and the core has the expected structural parameters.[19f,19h,19i,19j,19m] The Mo centers in **1** adopt a distorted octahedral geometry completed by three sulfur atoms and one bridging and two terminal oxygen atoms. The O_t–Mo–O_b angles range from 104.3(7)° to 105.8(8)°. The two Mo atoms are bridged by a single oxygen atom (Mo1–O1 = 1.91(1) and Mo2–O1 = 1.86(1) Å).

Two sets of three bridging μ-SCH_3 ligands are disposed in the anti-clockwise (for the μ-SCH_3 ligands bridging Rh(1)···Mo(1)) or in the clockwise (for those bridging Rh(2)···Mo(2)) orientations with respect to the methyl groups, when one views along the Rh···Mo axes from the Rh sites (complex **1** is a kind of diastereoisomers toward either enantiomer of (anti & anti) and (clockwise & clockwise)).

It is found that the intramolecular contacts between methyl groups and terminal oxo atoms: C23···O2 = 3.12(3) Å, C22···O3 = 3.02(3) Å, C25···O4 = 3.08(3) Å, and C26···O5 = 2.96(3) Å. These interatomic distances are below the sum of the van der Waals radii (3.4 Å).

Molecular Structure of 2 and 3. As shown in Figs. 2 and 3 complexes **2** and **3** have an analogous structure in a *syn* arrangement, but they have the different bridging atoms: a di(μ-oxo)dimolybdenum(V) core in **2** and a (μ-oxo)(μ-sulfido)dimolybdenum(V) one in **3**. The diamagnetic nature of **2** and **3** is accounted for by strong interactions between two Mo^V centers (d^1–d^1) with the Mo–Mo distances of 2.564(1) Å for **2** and 2.666(1) Å for **3**. The structure parameters of the cores fall within the range of those for the dimolybdenum complexes whose structures were confirmed by X-ray analyses to date.[19a,19b,19c,19e,19h,19i,19j,19l,19m]

The three μ-SCH_3 ligands bridge the Rh and Mo centers to form the $Cp^*Rh(\mu\text{-}SCH_3)_3MoO$ moieties with the Rh···Mo distances of 3.466(2) and 3.471(1) Å for **2** and 3.480(1) and 3.477(1) Å for **3**. For both complexes two sets of the three μ-SCH_3 ligands are disposed in the anti-clockwise direction with respect to the Rh···Mo axes. Their enantiomers with clockwise arrangements equally exist in the crystals. The Rh–S(CH_3) distances are shorter compared to the Mo–S(CH_3) distances: the Rh–S(CH_3) distances range from 2.351(2) to 2.391(3) Å and the Mo–S(CH_3) distances 2.548(2) to 2.736(3) Å for **2**. The same tendency is observed for **3** (the Rh–S(CH_3) distances of 2.360(2)—2.379(2) Å and the Mo–S(CH_3) distances of 2.556(2)—2.734(2) Å). The Mo–S(CH_3) bonds trans to the terminal oxygen atoms are longer by ca. 0.1—0.2 Å compared to those trans to the bridging oxygen or sulfur atoms, which is due to the stronger trans influence of the terminal oxygen atoms.

As observed in **1**, intramolecular contacts between the methyl groups and terminal oxo, bridging oxo and bridging sulfido ligands are also seen for **2** and **3**. The average interatomic distances are the C···O_t = 3.02 Å and C···O_b = 3.16 Å for **2**, and the C···O_t = 3.03 Å, C···O_b = 3.10 Å, and C···S_b = 3.39 Å for **3**.

NMR Studies. Solution properties of the tetranuclear complexes have been investigated by ^1H, ^{13}C, and ^{17}O NMR spectroscopy. Variable-temperature ^1H and ^{13}C NMR spectroscopy indicates that these tetranuclear complexes are fluxional in nonaqueous media ($CDCl_3$, CD_2Cl_2, $C_2D_4Cl_2$, $C_2D_2Cl_4$, $C_6D_5NO_2$, and C_6D_5Cl). Line-shape analysis of the ^1H NMR signals of μ-SCH_3 for complexes **2** and **3** was carried out using a computer program based on a modified Bloch equation with the three-site exchange model[15] and using the spectrum measured in C_6D_5Cl at 10 °C as the low-temperature limit spectrum (the static spectrum).

In the case of **3**, two specific sets of μ-SCH_3 resonances (comprising of three singlets each) were determined by trial-and-error procedures so as to reproduce the observed spectra with a given rate constant in the whole temperature range (10 to 120 °C). In this way, the two sets of three singlets at δ = 2.86 (resonance d), 2.83 (f), and 2.07 (i) and those at δ = 2.85 (e), 2.69 (g), and 2.13 (h) were taken as the exchange couples (see Fig. 4 with the signal labeling: Almost the same results was obtained from the line shape analyses of either set).

At lower temperatures, **2** and **3** show simple NMR spectral patterns as expected from the crystal structures. While **1** exists as two isomers in solution,[8] one of which is consistent with the species found in the crystal structure. Unfortunately, we do not have any structural information of the other species. Both isomers show concerted and complicated line broadening in ^1H NMR signals of μ-SCH_3. Thus, we discuss here the solution dynamic properties only for **2** and **3**.

Variable-Temperature ^1H NMR Spectra. ^1H NMR spectra of the methyl region for **2** and **3** in C_6D_5Cl at 10 °C are shown in Fig. 4 with the signal numbering. Due to the existence of the pseudo two-fold axis through the center of the plane surrounded by the $Mo_2(\mu\text{-}O)_2$, **2** shows only three singlets from the μ-SCH_3 ligands at δ = 2.84 (resonance a), 2.56 (b), and 2.08 (c) with the equal intensity, and an addi-

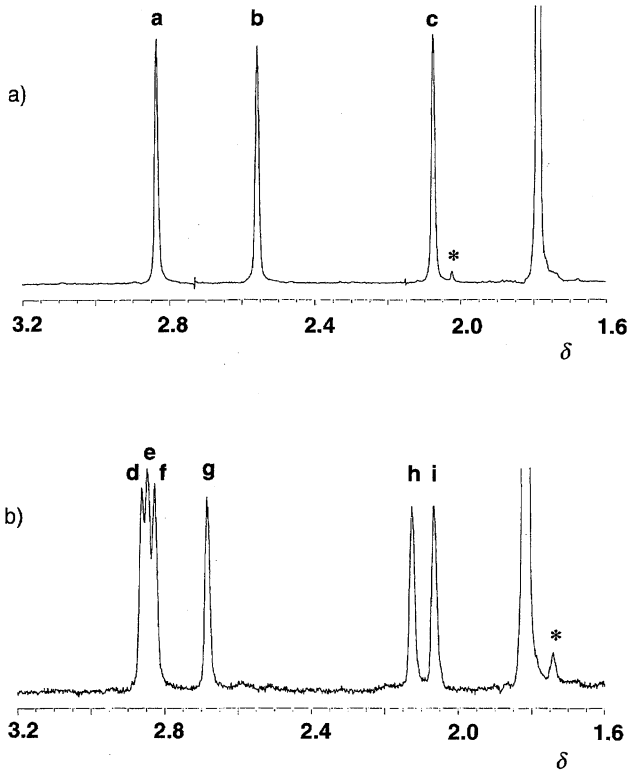

Fig. 4. ^1H NMR spectra of [{$Cp^*Rh(\mu\text{-}SCH_3)_3MoO$}$_2$-($\mu$-O)$_2$] (**2**) (a) and [{$Cp^*Rh(\mu\text{-}SCH_3)_3MoO$}$_2$($\mu$-O)-($\mu$-S)] (**3**) (b) in C_6D_5Cl at 10 °C with signal numbering scheme. Resonances at δ = 1.78 for **2** and δ = 1.81 for **3** are due to Cp^* methyl groups. Signals with * are due to impurities.

tional singlet from the Cp^* rings at $\delta = 1.78$ (Fig. 4a). In the case of **3** that has two different bridging ligands between Mo atoms (O and S), all μ-SCH_3 ligands are nonequivalent and thus six singlets are observed at $\delta = 2.86$ (resonance d), 2.85 (e), 2.83 (f), 2.69 (g), 2.13 (h), and 2.07 (i), along with a Cp^* singlet at $\delta = 1.81$ (Fig. 4b). This chemically nonequivalent nature for the methyl groups indicates that no methyl inversion at the sulfur centers[21] of μ-SCH_3 occurs. Higher-temperature ^{1}H NMR spectra of complexes **2** and **3** in C_6D_5Cl are displayed in the left side of Figs. 5 and 6, respectively. With increasing temperature, the three separated μ-SCH_3 resonances in **2** at lower temperatures broaden until they coalesce to give a single broad resonance at 90 °C (δ = ca. 2.5). At higher temperatures, more sharp resonance is obtained. For **3**, the line-broadening becomes evident at about 60 °C, and as temperature increases further, the six signals collapse and merge into a single peak at δ = ca. 2.6 over 80 °C. This temperature-dependent behavior is fully reversible.

This averaging process can be explained by assuming that intramolecular rotations of the "$Cp^*Rh(\mu$-$SCH_3)_3$" fragments occur about the Mo centers, not by the methyl inversion which may leads to the different spectral changes from those shown in Figs. 5 and 6: The three signals in **2** do not coalese with one another and the six signals in **3** merge into three signals by this inversion. This fluxional behavior may be approximated to a three-site exchange process with equally populated, uncoupled sites.[15] Calculated spectra and rate constants are shown in the right side of Figs. 5 and 6. In the case of **3**, two specific combinations of three exchange singlets are chosen for the analysis as mentioned before. Eyring plots are shown in Fig. 7, giving good straight lines for both complexes. Activation parameters and rate constants are tabulated in Table 3. It is apparent that almost the same values are obtained for **2** and **3**; activation enthalpies lie in the range +68.7 to +80.2 kJ mol^{-1}, while the activation entropies show relatively small negative or positive values, -11.3 to +22.3 J K^{-1} mol^{-1}. It seems that activation parameters are not dependent on solvents used. The small entropic contributions strongly suggest that the exchange process is intramolecular.

^{17}O NMR. To gain more insight into the solution be-

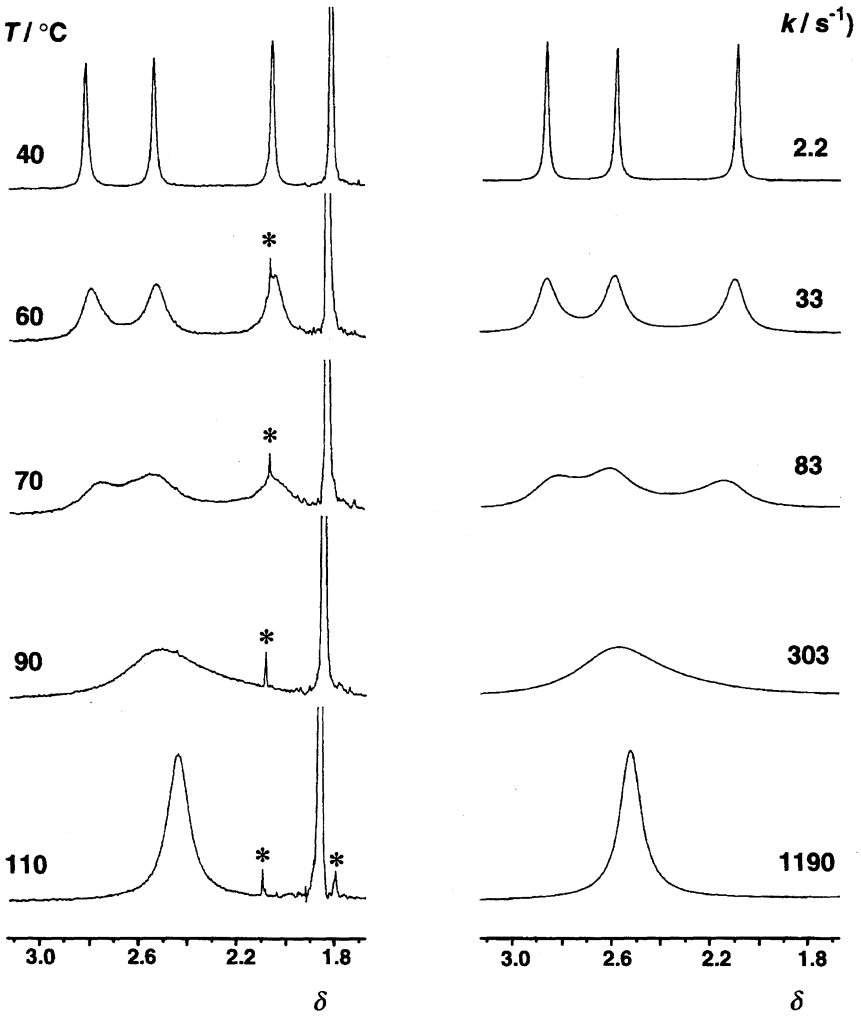

Fig. 5. Observed (left) and calculated (right) ^{1}H NMR spectra of [{$Cp^*Rh(\mu$-$SCH_3)_3MoO\}_2(\mu$-$O)_2$] (**2**) in C_6D_5Cl at various temperatures together with rate constants. A resonance at δ = ca. 1.8 is due to Cp^* methyl groups. Signals with * are due to impurities.

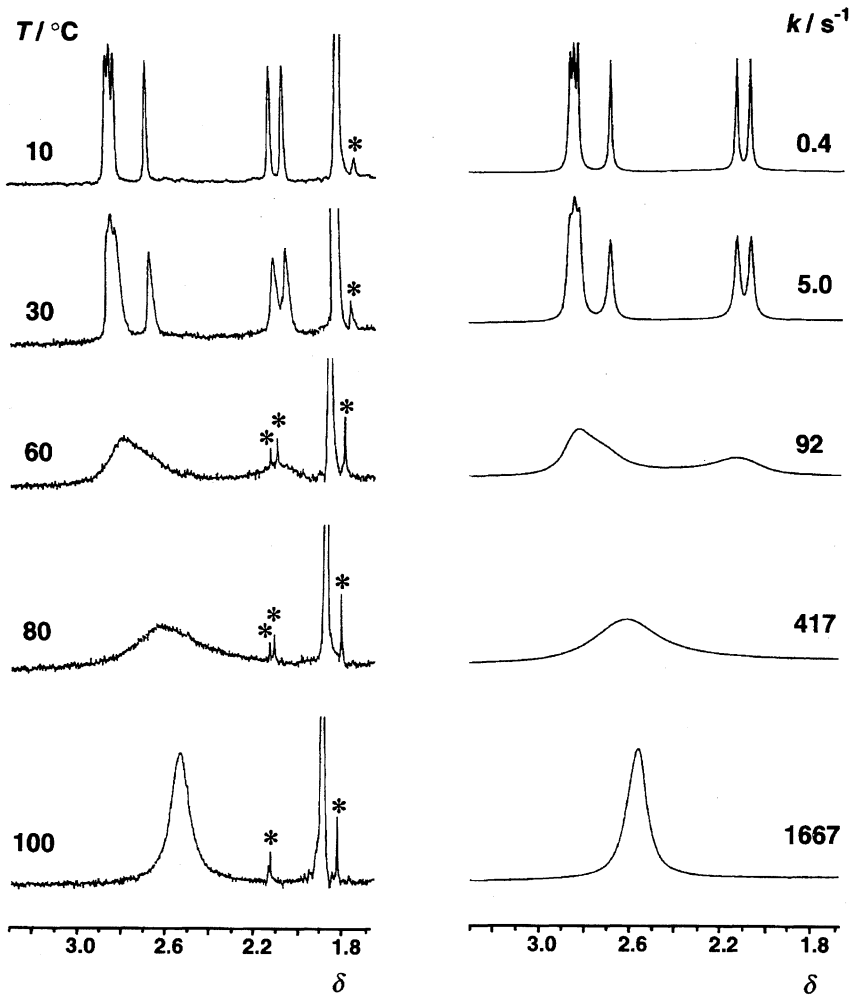

Fig. 6. Observed (left) and calculated (right) ^{1}H NMR spectra of [{Cp*Rh(μ-SCH$_3$)$_3$MoO}$_2$(μ-O)(μ-S) (**3**) in C_6D_5Cl at various temperatures together with rate constants. A resonance at δ = ca. 1.8 is due to Cp* methyl groups. Signals with * are due to impurities.

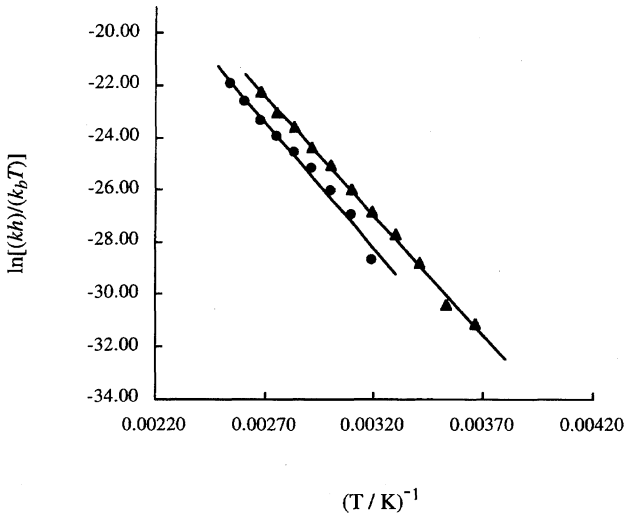

Fig. 7. Eyring plots for **2** (●) and **3** (▲) (solvent: C_6D_5Cl).

havior of **2** and **3**, ^{17}O NMR spectra were measured for the ^{17}O-enriched complexes of **2′** and **3′**.

Complexes **2′** and **3′** exhibit two and three ^{17}O-singlets, respectively (Fig. 8), as expected from their crystal structures. The assignments are made on the basis of the established correlations between higher-field shift of ^{17}O-resonances and longer metal–oxygen bond distance (Table 4).[22] In $CDCl_3$ two singlets of **2′** at δ = 940 ($W_{1/2}$ = 253 Hz) and 598 ($W_{1/2}$ = 349 Hz) with the almost equal integrated intensity can be assigned to the terminal Mo–O$_t$ oxygens and the bridging Mo–O$_b$–Mo oxygen, respectively. In $CDCl_3$ three singlets in **3′** consist of two singlets for the terminal oxygens at δ = 956 ($W_{1/2}$ = 304 Hz) and 947 ($W_{1/2}$ = 324 Hz) and one singlet for the bridging oxygen at δ = 582 ($W_{1/2}$ = 399 Hz). These ^{17}O NMR spectral patterns clearly demonstrate that the dinuclear Mo frameworks of OMo(μ-X)(μ-Y)MoO (X = Y = O for **2′** and X = O, Y = S for **3′**) are retained in solution. The important thing is that no significant spectral change with temperature (23 to 120 °C in $C_6D_5NO_2$) was observed for either complex, except for the quadrupolar line-narrowing with increasing temperature.

Mechanism of Dynamic Process. From the results of the successful line-shape fitting by using the three-site exchange model and the ^{17}O NMR spectroscopic study mentioned above, the averaging process of three or six meth-

Table 3. Activation Parameters and Rate Constants for [{Cp*Rh(μ-SCH_3)$_3$MoO}$_2$(μ-O)$_2$] (**2**) and [{Cp*Rh(μ-SCH_3)$_3$MoO}$_2$(μ-O)(μ-S)] (**3**)

Complex	Solvent	$\Delta H^{\ddagger}$/kJ mol^{-1}	$\Delta S^{\ddagger}$/J K^{-1} mol^{-1}	$\Delta G^{\ddagger}_{298\,K}$/kJ mol^{-1}
2	$CDCl_3$	+72.4±1.2	+1.7±0.3	+71.9
	C_6D_5Cl	+80.2±3.7	+22.1±2.3	+73.6
	$C_2D_2Cl_4$	+68.7±0.5	−11.3±0.4	+72.1
3[a)]	$CDCl_3$	+73.9±2.4	+22.3±0.7	+67.3
	C_6D_5Cl	+76.8±1.7	+21.1±1.4	+70.5

a) Since this complex was unstable in $C_2D_2Cl_4$ at elevated temperature, the activation parameters were obtained only for $CDCl_3$ and C_6D_5Cl solutions.

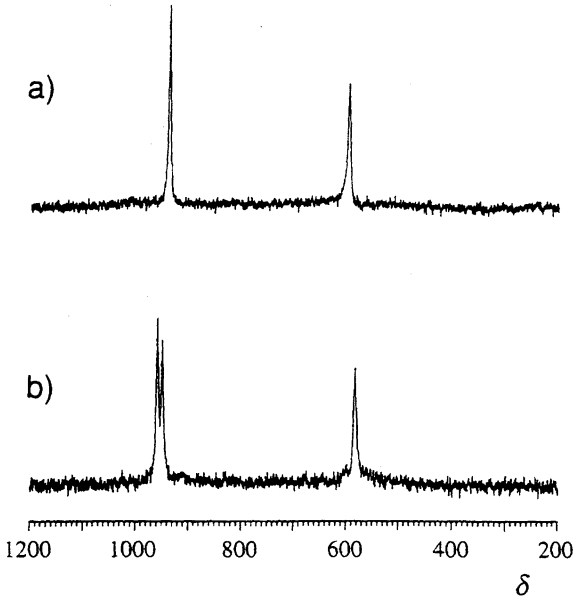

Fig. 8. ^{17}O NMR spectra of **2′** (a) and **3′** (b) in $CDCl_3$ at 23 °C.

Table 4. ^{17}O NMR Data for **2′** and **3′** at 23 °C

Complex	Solvent	Chemical shift[a)]/ppm [$W_{1/2}$/Hz]	
		Mo–O_t	Mo–O_b–Mo
2′	$CDCl_3$	940 [253]	598 [349]
	$C_2D_2Cl_4$	933 [806]	606 [875]
3′	$CDCl_3$	956 [304]	
		947 [324]	582 [399]
	$C_2D_2Cl_4$	949 [1125]	587 [758]

a) Chemical shifts are referenced to D_2O externally by the sample replacement method.

yl resonances of **2** or **3** may be best described by the intramolecular rotations of the "Cp*Rh(μ-SCH_3)$_3$" moieties on the trigonal planes of the octahedral Mo centers. The pyramidal inversions of methyl groups at the sulfur centers, which are seen in tri(μ-SCH_3) complexes of [(η^7-$C_7H_3R^1{}_4$)-Mo(μ-SR^2)$_3$Mo(η^7-$C_7H_3R^1{}_4$)] (R^1 = H or CH_3; R^2 = C_2H_5, $(CH_2)_2CH_3$, $(CH_2)_3CH_3$, C_6H_5 or $CH_2C_6H_5$),[23a] [L_3Mo-

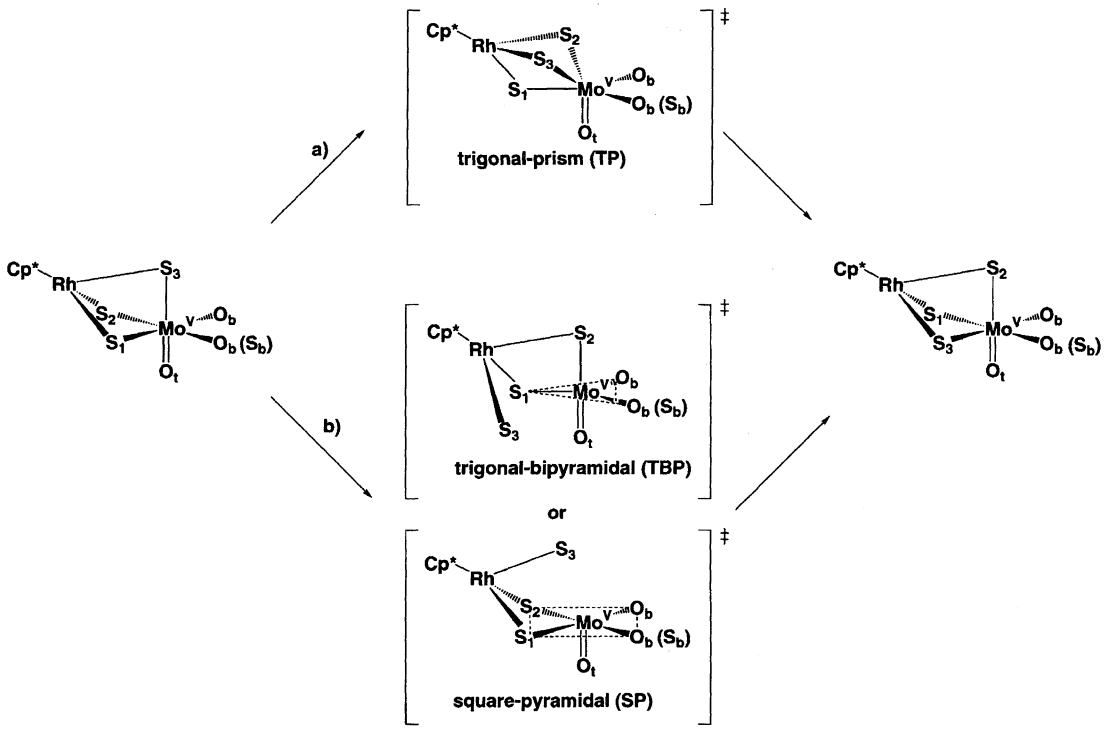

Scheme 3.

(μ-SC(CH$_3$)$_3$)$_3$Mo(η^7-C$_7$H$_7$)] (L = P(OCH$_3$)$_3$, P(CH$_3$)(C$_6$H$_5$)$_2$, P(CH$_3$)$_2$(C$_6$H$_5$), P(CH$_3$)$_3$),[23b] and [(CO)$_3$Mo(μ-SR)$_3$Mo(η^7-C$_7$H$_7$)] (R = CH$_3$, C$_2$H$_5$, CH(CH$_3$)$_2$ or C(CH$_3$)$_3$)[23c] and have relatively small activation free energy ($\Delta G^{\ddagger}$) values around 50 kJ mol^{-1}, cannot explain the observed spectral changes. Possible intramolecular rearrangement processes for the present system are illustrated in Schemes 3a and 3b, based on the twist mechanism and the bond-rupture mechanism,[24] respectively. In the transition state, the former involves a six-coordinate trigonal prism (TP) Mo center, while the latter involves a five-coordinate trigonal bipyramidal (TBP) or a square pyramidal (SP) Mo center. Judging from the activation parameters (not so large $\Delta G^{\ddagger}$ values and small $\Delta S^{\ddagger}$ values, Table 3), the twist mechanism, Scheme 3a, seems to be more likely. Interestingly, it has been found that the μ-SR (R = CH$_3$ and C$_6$H$_5$) ligand in [Cp$_2$Mo$_2$(μ-SR)(CO)$_4$]$^-$ on its *trans–trans* interconversion shows a very similar motion[25] to that for the individual μ-SCH$_3$ ligand in **2** or **3** when the twist mechanism works in the fluxional behaviors. However, the bond-rupture mechanism (Scheme 3b), which was found in the *cis–trans* isomerization of [Cp$_2$Fe$_2$(CO)$_2$(μ-SC$_6$H$_5$)$_2$],[21b] still cannot be ruled out at this stage. It is possible that the rotation of the Rh fragments is initiated by the cleavage of the Mo–S bond trans to the terminal oxo ligands. This bond is longer by ca. 0.1 to 0.2 Å compared to the other two Mo–S bonds and may easily be cleaved in transition states.

Conclusion

Each reaction of the triple cubane-type cluster [(Cp*Rh)$_4$Mo$_4$O$_{16}$] with CH$_3$OH, 1,2-C$_6$H$_4$(SH)$_2$, or CH$_3$SH brings about the rearrangement of the cluster framework in a different way.[6—10] The CH$_3$OH molecule performs moderately the metal–oxygen bond rearrangement maintaining the cubic M$_4$O$_4$ framework. On the other hand, 1,2-C$_6$H$_4$(SH)$_2$ reconstructs the cluster framework, separating the organorhodium and oxide parts. The reactivity of the CH$_3$SH molecule is intermediate between them. Under certain reaction conditions described in this paper, the reactions with CH$_3$SH give three linear-type tetranuclear complexes **1**—**3**, which contain both two Mo and two Rh atoms. This may come from the differences in pK_a, coordination ability to the Rh and Mo atoms, and the bond energy of C–X (X = O, S) among CH$_3$OH, 1,2-C$_6$H$_4$(SH)$_2$, and CH$_3$SH.

These tetranuclear complexes were characterized and the solution dynamic properties of **2** and **3** were examined by line-shape analysis of the ^{1}H NMR signals of μ-SCH$_3$ using a modified Bloch equation with the three-site exchange model[15] and reasonably accounted for by the unique intramolecular rotation of the Cp*Rh(μ-SCH$_3$)$_3$ fragments on the trigonal planes of the Mo centers. This is the first example of complete averaging of triply-bridging μ-SCH$_3$ ligands in complexes in solution.

Supporting Information Available: Full crystallographic data and refinement parameters, atomic coordinates, listings of bond distances and angles, anisotropic displacement parameters for **1**—**3** are deposited as Document No. 72031 at the Office of the Editor of Bull. Chem. Soc. Jpn.

This work was supported by a Grant-in-Aid for Scientific Research on Priority Areas Nos. 10149101 and 09239104 from the Ministry of Education, Science, Sports and Culture. We are grateful to Dr. Shigetaka Koda (Fujisawa Pharmaceutical Company) for the X-ray data collection of **1**.

References

1 a) C. L. Hill, *Chem. Rev.*, **98**, 1 (1998). b) K. Isobe and A. Yagasaki, *Acc. Chem. Res.*, **26**, 524 (1993). c) F. Bottomley and L. Sutin, *Adv. Organomet. Chem.*, **28**, 339 (1988). d) V. W. Day and W. G. Klemperer, *Science*, **228**, 533 (1985).

2 a) M. Ichikawa, W. Pan, Y. Imada, M. Yamaguchi, K. Isobe, and T. Shido, *J. Mol. Catal., A*, **107**, 23 (1996). b) C. Zhang, Y. Ozawa, Y. Hayashi, and K. Isobe, *J. Organomet. Chem.*, **373**, C21 (1989). c) Y. Iwasawa, "Catalysis by Metal Complexes: Tailored Metal Catalysts," Reidel, Dordrecht, The Netherlands (1986).

3 a) G. Süss-Fink, L. Plasseraud, V. Ferrand, S. Stanislas, A. Neels, H. Stoeckli-Evans, M. Henry, G. Laurenczy, and R. Roulet, *Polyhedron*, **17**, 2817 (1998). b) K. Nomiya, C. Nozaki, A. Kano, T. Taguchi, and K. Ohsawa, *J. Organomet. Chem.*, **533**, 153 (1997). c) Y. Hayashi, F. Müller, Y. Lin, S. M. Miller, O. P. Anderson, and R. G. Finke, *J. Am. Chem. Soc.*, **119**, 11401 (1997). d) V. W. Day, W. G. Klemperer, and D. J. Main, *Inorg. Chem.*, **29**, 2345 (1990). e) R. G. Finke, D. K. Lyon, K. Nomiya, S. Sur, and N. Mizuno, *Inorg. Chem.*, **29**, 1784 (1990). f) H. K. Chae, W. G. Klemperer, and V. W. Day, *Inorg. Chem.*, **28**, 1423 (1989).

4 a) S. Takara, T. Nishioka, I. Kinoshita, and K. Isobe, *J. Chem. Soc., Chem. Commun.*, **1997**, 891. b) M. Abe, K. Isobe, K. Kida, and A. Yagasaki, *Inorg. Chem.*, **35**, 5114 (1996). c) M. Abe, K. Isobe, K. Kida, A. Nagasawa, and A. Yagasaki, *J. Cluster Sci.*, **5**, 565 (1994). d) Y. Hayashi, Y. Ozawa, and K. Isobe, *Inorg. Chem.*, **30**, 1025 (1991). e) H. Akashi, K. Isobe, Y. Ozawa, and A. Yagasaki, *J. Cluster Sci.*, **2**, 291 (1991). f) Y. Hayashi, Y. Ozawa, and K. Isobe, *Chem. Lett.*, **1989**, 425.

5 Y. Hayashi, K. Toriumi, and K. Isobe, *J. Am. Chem. Soc.*, **110**, 3666 (1988).

6 Y. Do, X.-Z. You, C. Zhang, Y. Ozawa, and K. Isobe, *J. Am. Chem. Soc.*, **113**, 5892 (1991).

7 R. Xi, M. Abe, T. Suzuki, T. Nishioka, and K. Isobe, *J. Organomet. Chem.*, **549**, 117 (1997).

8 R. Xi, B. Wang, Y. Ozawa, M. Abe, and K. Isobe, *Chem. Lett.*, **1994**, 323.

9 R. Xi, B. Wang, M. Abe, Y. Ozawa, and K. Isobe, *Chem. Lett.*, **1994**, 1177.

10 R. Xi, B. Wang, K. Isobe, T. Nishioka, K. Toriumi, and Y. Ozawa, *Inorg. Chem.*, **33**, 833 (1994).

11 R. Xi, Ph.D. Thesis (No. Kou-122-Go), 1995, "Transformation of Framework of Triple Cubane-Type Rh–Mo Oxide Cluster by Using Mercaptans: Dynamic Behavior of Linear-Type Tetranuclear Complexes in Solution," The Graduate University for Advanced Studies, Hayama, Japan. The preparation and X-ray analysis of [(Cp*Rh)$_2$(μ-SCH$_3$)$_3$]$_2$[Mo$_6$O$_{19}$] are reported in the thesis.

12 C. White, A. Yates, and P. M. Maitlis, *Inorg. Synth.*, **29**, 228 (1992).

13 This solid appears to contain polyoxometalates of [(Cp*Rh)$_2$(μ-SCH$_3$)$_3$]$_4$[Mo$_8$O$_{26}$][10] and [(Cp*Rh)$_2$(μ-SCH$_3$)$_3$]$_4$-[Mo$_6$O$_{19}$][11] on the basis of IR spectra.

14 a) G. M. Sheldrick, C. Kruger, and R. Goddard, "Crystal-

lographic Computing 3," Oxford University Press, Oxford (1985), pp. 175—189. b) T. Sakurai and K. Kobayashi, *Rigaku Kenkyusho Hokoku*, **55**, 69 (1979).

15 J. Sandström, "Dynamic NMR Spectroscopy," Academic Press, Yew York (1982), pp. 18—25.

16 Dimethyl sulfide $(CH_3S)_2$ was detected by ^{1}H NMR spectrum (δ = 2.40) for the CD_3OD solution containing $[(Cp^*Rh)_4Mo_4O_{16}]$ and CH_3SH.

17 pK_a = 10.7 for CH_3SH (J. A. Dean, "Lange's Handbook of Chemistry," 14th ed, McGraw-Hill, Inc., New York (1992), Sects. 8, 8.19) and pK_a = 15.5 for CH_3OH (J. A. Riddick, W. B. Bunger, and T. K. Sakano, "Techniques of Chemistry," 4th ed, John Wiley & Sons, New York (1986), Vol. 2, Organic Solvents, p. 191).

18 a) W. D. Jones and R. M. Chin, *J. Am. Chem. Soc.*, **116**, 198 (1994). b) B. C. Wiegand and C. M. Friend, *Chem. Rev.*, **92**, 491 (1992). c) S. Luo, A. E. Ogilvy, T. B. Rauchfuss, A. L. Rheingold, and S. R. Wilson, *Organometallics*, **10**, 1002 (1991). d) C. M. Friend and J. T. Roberts, *Acc. Chem. Res.*, **21**, 394 (1988). e) R. J. Angelici, *Acc. Chem. Res.*, **21**, 387 (1988).

19 a) H. Adams, L. J. Gill, and M. J. Morris, *J. Chem. Soc., Dalton Trans.*, **1998**, 2451. b) M. Cindric, D. M. Calogovic, V. Vrdoljak, and B. Kamenar, *Struct. Chem.*, **9**, 353 (1998). c) R. Hazama, K. Umakoshi, A. Ichimura, S. Ikari, Y. Sasaki, and T. Ito, *Bull. Chem. Soc. Jpn.*, **68**, 456 (1995), see several references therein. d) K. Unoura , Y. Fukase, Y. Sato, N. Chida, and H. Ogino, *Bull. Chem. Soc. Jpn.*, **67**, 3122 (1994). e) T. Shibahara, *Coord. Chem. Rev.*, **123**, 73 (1993). f) K. S. Bürger, G. Haselhorst, S. Stötzel, T. Weyhermüller, K. Wieghardt, and B. Nuber, *J. Chem. Soc., Dalton Trans.*, **1993**, 1987. g) R. H. Holm, *Coord. Chem. Rev.*, **100**, 183 (1990). h) F. A. Cotton and G. Wilkinson, "Advanced Inorganic Chemistry," 5th ed, John Wiley & Sons, New York (1988), pp. 824—831. i) C. D. Garner and J. M. Charnock, "Comprehensive Coordination Chemistry," ed by G. Wilkinson, R. D. Gillard, and J. A. McCleverty, Pergamon Press, Oxford (1987), Vol. 3, Part 36.4, pp. 1329—1374 and E. I. Stiefel, Vol. 3, Part 36.5, pp. 1375—1420. j) R. H. Holm, *Chem. Rev.*, **87**, 1401 (1987). k) K. Saito and Y. Sasaki, *Adv. Inorg. Bioinorg. Mech.*, **1**, 179 (1982). l) E. I. Stiefel, *Prog. Inorg. Chem.*, **22**, 1 (1977). m) B. Spivack and Z. Dori, *Coord. Chem. Rev.*, **17**, 99 (1975).

20 S. Stötzel, K. Wieghardt, and B. Nuber, *Inorg. Chem.*, **32**, 2128 (1993).

21 a) E. W. Abel, S. K. Bhargava, and K. G. Orrell, *Prog. Inorg. Chem.*, **32**, 1 (1984). b) S. D. Killops and S. A. R. Knox, *J. Chem. Soc., Dalton Trans.*, **1978**, 1260. c) E. W. Abel, G. W. Farrow, K. G. Orrell, and V. Sik, *J. Chem. Soc., Dalton Trans.*, **1977**, 42.

22 a) C. J. Besecker, W. G. Klemperer, D. J. Maltbie, and D. A. Wright, *Inorg. Chem.*, **24**, 1027 (1985). b) M. Filowitz, R. K. C. Ho, W. G. Klemperer, and W. Shum, *Inorg. Chem.*, **8**, 93 (1979). c) W. G. Klemperer, *Angew. Chem., Int. Ed. Engl.*, **17**, 246 (1978).

23 a) M. L. H. Green and D. K. R. Ng, *J. Chem. Soc., Dalton Trans.*, **1993**, 11. b) I. B. Benson, S. A. R. Knox, P. J. Naish, and A. J. Welch, *J. Chem. Soc., Dalton Trans.*, **1981**, 2235. c) I. B. Benson, S. A. R. Knox, P. J. Naish, and A. J. Welch, *J. Chem. Soc., Chem. Commun.*, **1978**, 878.

24 a) J. D. Atwood, "Inorganic and Organometallic Reaction Mechanisms," 2nd ed, VCH, New York (1997), Chap. 7, pp. 231—271. b) R. H. Holm, "Dynamic Nuclear Magnetic Resonance Spectroscopy," ed by L. M. Jackman and F. A. Cotton, Academic Press, New York (1975), pp. 317—376. c) C. S. Springer, Jr., *J. Am. Chem. Soc.*, **95**, 1459 (1973). d) J. G. Gordon, II, and R. H. Holm, *J. Am. Chem. Soc.*, **92**, 5319 (1970). e) E. L. Muetterties, *J. Am. Chem. Soc.*, **90**, 5097 (1968). f) C. S. Springer, Jr., and R. E. Sievers, *Inorg. Chem.*, **6**, 852 (1967).

25 P. Schollhammer, F. Y. Pétillon, S. Poder-Guillou, J. Talarmin, K. W. Muir, and D. S. Yufit, *J. Organomet. Chem.*, **513**, 181 (1996).